ELSEVIER

Journal of Non-Crystalline Solids 284 (2001) 174–182

JOURNAL OF NON-CRYSTALLINE SOLIDS

www.elsevier.com/locate/jnoncrysol

Ironporphyrins trapped sol–gel glasses: a chemometric approach

Hérica C. Sacco [a,b], Katia J. Ciuffi [c], Juliana C. Biazzotto [b], Cesar Mello [c], Daniela C. de Oliveira [c], Ednalva A. Vidoto [a,b], Otaciro R. Nascimento [a], Osvaldo A. Serra [b], Yassuko Iamamoto [b,*]

[a] *Instituto de Física de São Carlos, USP, São Carlos, SP, Brazil*

[b] *Universidade de São Paulo, FFCLRP-USP, Departmento de Química, Av. Bandeirantes 3900, CEP 14040-901, Rib. Preto, SP, Brazil*

[c] *Universidade de Franca, Franca, SP, Brazil*

Abstract

The optimised conditions for preparation of ironporphyrin (FeP)-template trapped silica obtained by the sol–gel process are analysed by fractional factorial design. The FeP iron 5,10,15,20-tetrakis(pentafluorophenyl)-porphyrin (FeTFPPCl), iron 5,10,15,20-tetrakis(2,6-dichlorophenyl-3-sulphonatophenyl)-porphyrin (FeTDCSPP$(Na)_4$Cl), iron 5,10,15,20-tetrakis-*p*-carboxyphenylporphyrin (FeTCPP$(Na)_4$Cl) and iron 5,10,15,20-tetrakis-*p*-methylpyridilporphyrin (FeTMPyP$(Cl)_5$) were used. Pyridine or 4-phenylimidazole was used as template. Scanning electron microscopy (SEM) shows that the use of different porphyrins and conditions in the preparation of xerogel produce different product morphologies. The prepared materials have surface areas, between 300 and 1000 m^2/g. The electron paramagnetic resonance spectra of trapped materials have characteristic signal of Fe^{III} high spin, the presence of porphyrin species in a rhombic symmetry and porphyrin aggregates were also observed.

1. Introduction

One of the most recent application of the sol–gel method is the preparation of hybrid organic–inorganic materials which consist of polymers or organic molecules included in inorganic oxide networks [1]. The sol–gel process has been studied in the search for suitable matrices for catalyst immobilisation. In general, immobilisation methods include physical entrapment, covalent binding, or surface adsorption.

Hybrid materials containing the metalloporphyrin chemically bounded to the matrix through covalent bonds are proved to act as an efficient catalyst in oxidation reactions [2–7], even though their preparations are tedious. An easier possibility to obtain these materials in mild conditions is the inclusion of metalloporphyrins into porous silica by mixing the porphyrin precursor with a sol–gel colloid. After gelation, the organic molecules are entrapped in the porous matrix without covalent bond between the organic and inorganic fragments. The final material can be then used as catalyst in oxidation reactions, mimicking cytochrome P-450 [8].

The reaction to create a gel is complex and involves many variables; it has made the design and

* Corresponding author. Tel.: +55-16 602 3716; fax: +55-16 633 8151.

E-mail address: iamamoto@usp.br (Y. Iamamoto).

0022-3093/01/$ - see front matter
PII: S0022-3093(01)00398-2

control of xerogel properties an intricate task. The mechanism of entrapment of catalysts or organic molecules on the silica matrix is not yet fully understood [9] and manipulations of the key parameters of the glass formation process is of particular importance to investigate guest–host interactions, and to some extent, to control them. In fact, the degree of leaching of the entrapped molecule from the host matrix is strictly connected with the nano- and micro-structure of the final material (the relative size of the pores), and in consequence with the parameters which affect the rates of hydrolysis and condensation of alkoxisilane precursors. The importance of these variables in the xerogel process can be identified and analysed by fractional factorial design, which enables the efficient screening of variables, with a reduced number of experiments.

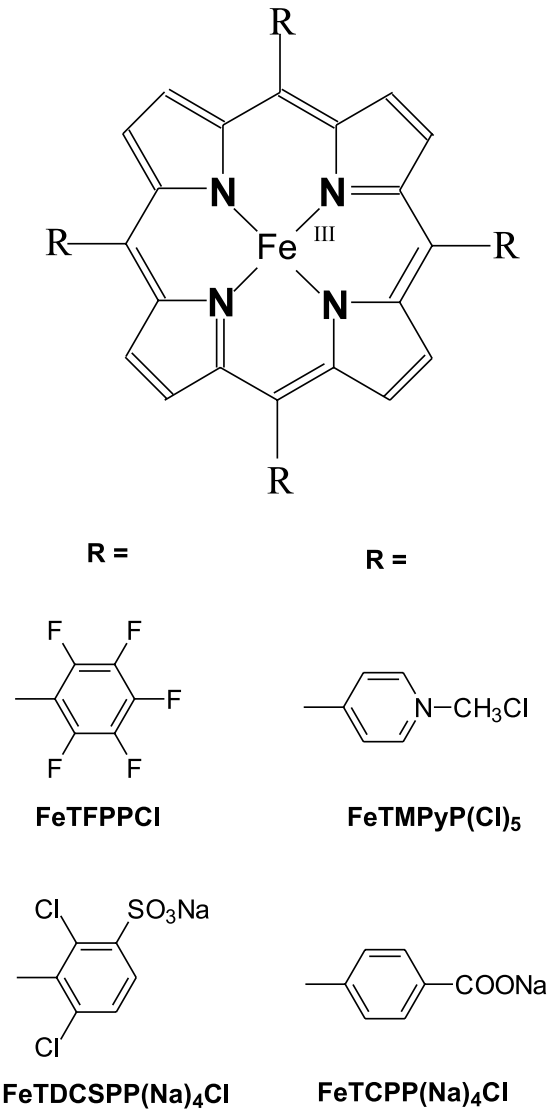

Fig. 1. Ironporphyrins.

In this paper, we describe the optimised conditions for preparation of ironporphyrin (FeP)-template trapped silica (Fe**PD**-template) obtained by the sol–gel process. The following FeP were used: FeTFPPCl, FeTDCSPP$(Na)_4Cl$, FeTCPP$(Na)_4Cl$ and FeTMPyP$(Cl)_5$ (Fig. 1). Pyridine or 4-phenylimidazole was used as template. Some of the variables that affect the loading of FeP on xerogel were identified and the magnitude of these variables that maximise the loading of FeP on xerogel were established through a chemometric approach. The studied variables were explored through a fractional factorial design in two levels, 2^{5-1} type, generating 16 total experiments for each FeP [10].

2. Experimental

2.1. Fractional factorial design

The investigated variables in this paper were solvent volume (A), water volume (B), reaction time (C), gelation temperature (D) and template (E). The choice of these variables was made considering the chemical characteristic of FeP systems (i.e., solvent was chosen considering FeP solubility, acid pH cause FeP demetallation and difficult template coordination, temperature maximum was kept at 120°C to avoid the rapid loose of reagents). The quantity of FeP and the choice of template (pyridine or 4-phenylimidazole) was based on previous works on supported FeP [11] and hybrid materials containing FeP [3–7]. All experiments were performed at 65% (±5%) relative air humidity. The alkoxide TEOS was chosen because it is one of the most studied sol–gel precursor [12], its availability and low cost. The chosen variables were explored through a fractional factorial design in two levels, 2^{5-1} type, generating 16 total

experiments for each FeP. The levels of the variables and the factorial design utilised are shown in Table 1 [10,13]. The fractional factorial design shown in Table 1 is a fractional factorial design with resolution 5, designated by 2_V^{5-1}. In this kind of factorial design the main effects are mixed only with the interactions of four factors, whereas the interactions of two factors are mixed with the interactions of three factors. Therefore, it is possible to suppose that interaction effects of three or more factors are insignificant to analyse only the main effects and the interaction effects of two factors [14]. The number of experiments was intentionally reduced in this study and we could not apply the principal component analysis (PCA) [15–20] to identify the relative influence of variables in the process. However we could identify some important variables estimating the effects of the factorial design on loadings. The calculation of the effects was obtained using a fractional factorial design program, written in Delphi® [21].

2.2. Metalloporphyrins

5,10,15,20-Tetrakis(2,6-dichlorophenyl-3-sulfonatophenyl)-porphyrin (H_2TDCSPP(Na_4)) and 5,10,15,20-tetrakis(pentafluororophenyl)-porphyrin (H_2TFPP) preparation and iron insertion were performed as described before [22–24]. Iron 5,10,15,20-tetrakis-*p*-carboxyphenylporphyrin (FeTCPP $(Na)_4Cl$) and iron 5,10,15,20-tetrakis-*p*-methylpyridilporphyrin (FeTMPyP$(Cl)_5$) were purchased from Midcentury.

2.3. Preparation of FeP trapped sol–gel materials

Initially the silica sol was prepared by stirring the solvent (ethanol or methanol), 3.0 ml of TEOS and water during 2 h, in the amounts given in Table 1. The FeP (3.0 mg) and 1×10^{-4} moles of template (pyridine or 4-phenylimidazole) were then added. The resulting solution was stirred for 3 or 9 days and allowed to stand under cover at 25°C or 120°C. The mixture becomes viscous and xerogels within 24 h when at 120°C and within ≈30 days when at 25°C, with a glassy aspect. The attained solid was ground and washed with methanol. The amount of FeP leached from silica material was quantified by measuring the FeP in the combined washings through ultraviolet–visible (UV–vis) spectroscopy.

The continuous-wave electron paramagnetic resonance (EPR) spectra of solids were performed using a commercial X-band spectrometer (Bruker Elexsys line E-580) equipped with standard rectangular cavity. Temperature at ~4 K was

Table 1
2^{5-1}- fractional factorial design for to estimate the effects and factor levels: solvent, volume, water volume, reaction time, temperature and template[a]

Experiment	Solvent volume (ml)	Water volume (ml)	Reaction time (h)	Temperature (°C)	Template
1	10	0.5	72	25	Pyridine
2	20	0.5	72	25	4-phim
3	10	3.0	72	25	4-phim
4	20	3.0	72	25	Pyridine
5	10	0.5	216	25	4-phim
6	20	0.5	216	25	Pyridine
7	10	3.0	216	25	Pyridine
8	20	3.0	216	25	4-phim
9	10	0.5	72	120	4-phim
10	20	0.5	72	120	Pyridine
11	10	3.0	72	120	Pyridine
12	20	3.0	72	120	4-phim
13	10	0.5	216	120	Pyridine
14	20	0.5	216	120	4-phim
15	10	3.0	216	120	4-phim
16	20	3.0	216	120	Pyridine

[a] 4-phim = 4-phenylimidazole.

controlled using a low temperature accessory (Helitran Oxford Systems). The EPR spectra of materials were recorded after adding 0.040–0.070 g of the dry material to an EPR quartz tube.

UV–visible spectra of solids were recorded in a UV–vis spectrophotometer (Hewlett-Packard 8453, Diode Array). The spectra of solids in suspension were recorded in a 2.0 mm path length cell. A better quality of spectra was obtained using dichloromethane (DCM) as solvent, where the suspension was prepared.

Specific surface area was determined by the BET method from nitrogen adsorption data using a Physical Adsorption Analyser Micrometrics AccSorb 2100 E [25].

Scanning electron microscopy (SEM) of FeP trapped materials were performed on a digital scanning microscope (DSM) (960 Zeiss).

3. Results

The FeP used in this study are presented in Fig. 1. Fe**PD** was prepared by the addition of a known quantity of FeP to a silica sol. After drying, the loading of FeP on silica was determined through repetitive washing of the attained material with methanol and the amount of leached FeP in the combined washings where measured by UV–vis spectroscopy. The effects of fractional factorial design on loadings obtained using FeTFPPCl, FeTCPP$(Na)_4$Cl and FeTDCSPP$(Na)_4$Cl are presented on Table 2, where l_x represents the effect of variable x ($x = A$ (solvent volume), B (water volume), C (reaction time), D (gelation temperature) and E (template)) on the loading of FeP on xerogel. l_x, $l_x > 0$, maximise the loading of FeP on xerogel, while $l_x < 0$ minimise the loading of FeP on xerogel.

Table 2
Effects of fractional factorial design on loadings obtained using FeTFPPCl, FeTCPP$(Na)_4$Cl and FeTDCSPP$(Na)_4$Cl

Contrasts (effects)	FeTFPPCl ± 0.4	FeTCPP$(Na)_4$Cl ± 0.5	FeTDCSPP$(Na)_4$Cl ± 0.5
l_A	0.8	−0.37	0.32
l_B	***−2.3***	***−2.1***	**−10.0**
l_C	***−2.5***	***−4.7***	−1.3
l_D	***5.0***	***6.7***	**12.0**
l_E	***−4.8***	***4.5***	**12.7**
l_{AB}	1.4	−1.6	−0.65
l_{AC}	0.08	0.31	−2.8
l_{AD}	1.05	1.4	2.1
l_{AE}	−0.9	−0.8	−0.4
l_{BC}	−0.8	1.4	1.1
l_{BD}	−0.03	−0.6	**−5.2**
l_{BE}	1.3	−0.3	**−7.0**
l_{CD}	***−2.0***	***−2.8***	−2.3
l_{CE}	***−2.0***	***−3.5***	−2.6
l_{DE}	**−2.3**	***−3.9***	**9.2**

Table 3
Properties of ironporphryrins trapped silica: loading of FeP, surface area, pore radius and pore volume

Material	Experiment	Loading (mg/g) ± 5	UV–vis (nm) ± 1	Surface area (m^2/g) ± 10	Pore radius (nm) ± 1	Pore volume (10^{-3} cm^3/g Å) ± 5
FeTFPP-py	11	2.2	434	691	2.1	70
FeTDCSPP-py	11	1.7	424	303	3.0	80
FeTCPP-py	11	17.7	420	389	15.6	15
FeTMPy-py	11	4.73	435	430	2.0	42
FeTMPy-4phim	14	34.3	435	508	1.5	38
FeTFPP-py	13	1.6	435	988	1.8	88
FeTDCSPP-4phim	9	7.6	430	327	1.9	26
FeTCPP-4phim	14	5.9	420	578	15.2	15

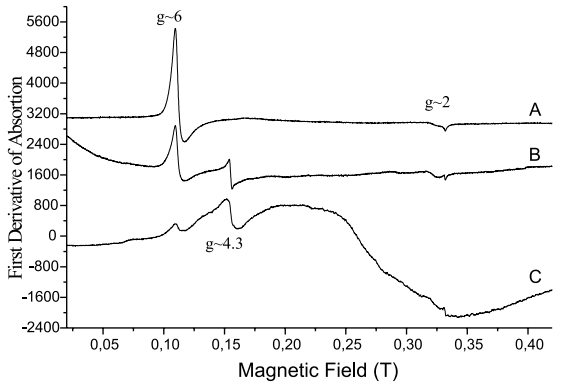

Fig. 2. EPR spectra of silica trapped containing FeTFPP: (a) Fe**PD**-pyridine loading 2.2 mg/g. (b) Fe**PD**-4-phenylimidazole loading 9.4 mg/g. (c) Fe**PD**-4-phenylimidazole loading 14.5 mg/g.

The UV–vis data, surface area and porosity relative to some of the prepared Fe**PD** materials are shown in Table 3. All UV–vis spectra of Fe**PD** contain the corresponding Soret band of homogeneous FeP [26].

EPR of FeTFPP trapped materials were measured. We observed the presence of Fe^{III} with typical g value at ~ 6 (Fig. 2), the presence of a signal at $g = 4.3$ due to various species of FeP in a rhombic symmetry [27,28] and a signal in the regions of 0.1500–0.3500 T of the spectra.

Fig. 3 shows the scanning electron micrographs of the prepared materials.

4. Discussion

To mimic cytochrome P450 and be useful as catalyst, trapped FeP prepared by sol–gel method should have catalytic activities and selectivities which are comparable to that of FeP in solution or supported by more traditional methods such as anchored on silica surface [11]. Usually, it is observed that anchored FeP show maximum catalytic activity when the FeP is in its Fe^{III} high spin state (spin = 3/2), with its sixth coordination site available for the oxidising agent [29,11]. In addition, good catalytic yields have been reported using the loading of FeP on matrix between 5 to 20 mg/g [2,3,11,30]. It was observed before by us that the amount of FeP loaded on silica can induce the formation of FeP aggregates with spin states other than 3/2, leading to low oxidation reaction yields [31].

The sol–gel preparation conditions are of importance for FeP entrapment. We already observed before that no FeP would be entrapped on silica for some conditions used [3–7]. Only $FeTMPyP(Cl)_5$ remained entrapped in the silica in all preparation conditions used and its loading varied between 3 to 34 mg/g. The presence of cationic groups in the $FeTMPyP(Cl)_5$ is responsible for the entrapment observed. For FeTFPP, $FeTDCSPP(Na)_4Cl$ and $FeTCPP(Na)_4Cl$ the loading of FeP on silica varied from 2 to 20 mg/g and the results obtained for all the contrasts on the loading for each FeP (effects for a fractional factorial design) are shown in the Table 3.

The variables that have the largest affect on the range studied for FeTFPPCl and $FeTCPP(Na)_4Cl$ loading (Table 3, bold) are water volume (B), reaction time (C), temperature (D) and template (E). Only water volume (B) does not present interaction effect with other variables and was analysed isolated (l_B). The variables, reaction time (C), temperature (D) and template (E), present interaction effects of two factors and were analysed in simultaneously (l_{CD}, l_{CE}, l_{DE}). The conclusion follows: (i) larger water volumes affects negatively FeTFPPCl and $FeTDCSPP(Na)_4Cl$ loadings; (ii) higher temperature maximise FeP loading, however this effect will be increased when the sol–gel mixture is stirred during 72 h; (iii) higher temperature maximise FeP loading, however this effect will be increased when pyridine is used as template; (iv) FeP loading is larger when pyridine is used as template instead of 4-phenylimidazole, however this effect will be minimised when the gelation temperature is 120°C; (v) FeP loading is larger when pyridine is used as template instead of 4-phenylimidazole – however this effect will be minimised when the sol–gel mixture is stirred during 72 h. In general, to maximise FeP loading on xerogel, the sol–gel process should be carried out volumes of water $\cong 0.5$ ml, temperature 120°C, using pyridine as template and reaction time of 72 h. On the range evaluated, solvent volume is not a significant variable.

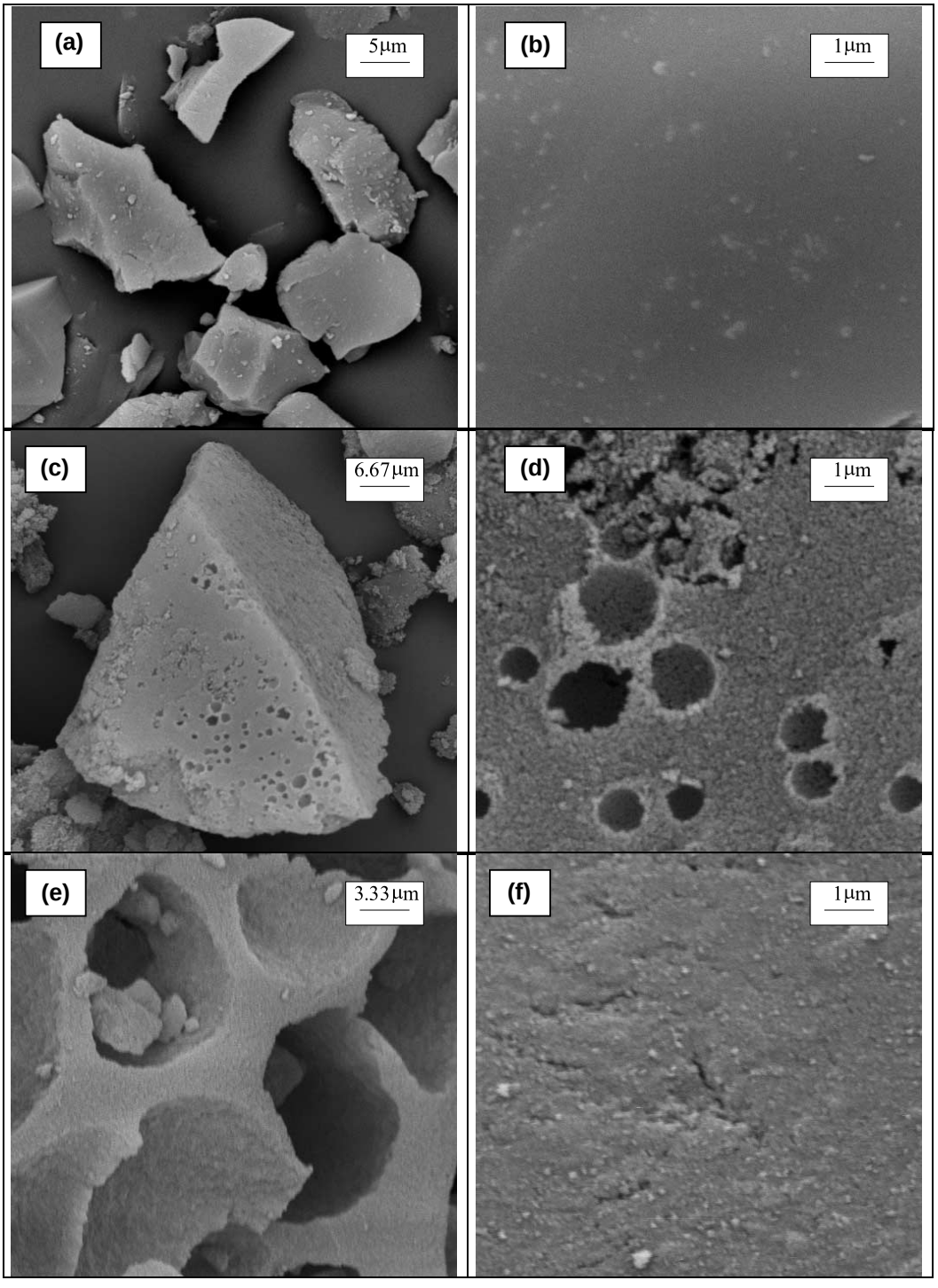

Fig. 3. SEM images of silica trapped with: (a) FeTDCSPP prepared at 120°C. (b) FeTDCSPP prepared at 25°C. (c) FeTCPP prepared at 120°C. (d) FeTFPP prepared at 120°C.

These results are valid only in the range of variables studied and the extrapolation to other situations not explored experimentally is not possible.

Identical analysis was carried out for FeTDCSPP$(Na)_4$Cl loading. To maximise FeP loading on xerogel, the sol–gel process should be carried out in volumes of water $\cong$0.5 ml, temperature 120°C, using 4-phenylimidazole as template. Solvent volume and reaction time are not significant variables on the range evaluated.

UV–vis spectra of Fe**P**-**D**-template samples had characteristic pattern of the corresponding FeP in solution [5], indicating that the structure of FeP was preserved in the xerogel matrix (Table 1). The Soret band of all Fe**P**-**D**-pyridine and 4-phenylimidazole is similar to that of Fe^{III}P in solution [26].

The analysis by EPR spectroscopy (Fig. 2) shows that even though for FeTFPPCl on experiment 11 the loading of FeP on silica was only 2.2 mg/g, the attained material presents only Fe^{III} high spin (spin = 3/2) with $g_{\perp} \sim 6$ and $g_{\parallel} \sim 2$ (Fig. 2(a)) [27,28]. The presence of a larger concentration of FeTFPPCl in the matrix to the formation of porphyrin aggregates, evidenced by the presence of a characteristic signal of zero field energy (Fig. 2(b)) [32,33] or a broad signal in the region of 0.1500–0.3500 T of the EPR spectra (Fig. 2(c)). We also observe the presence of porphyrin species in a rhombic symmetry, with $g \sim 4.3$ [27,28] (Fig. 2(b) and (c)). In general, we observed that entrapped FeTFPPCl with rhombic distortion (with EPR signal at $g \sim 4.3$) are formed when the sol containing the porphyrin is stirred during 216 h. Even though the loading of porphyrin FeTMPyP$(Cl)_5$ in the attained samples varied from 3.0 to 34.0 mg/g, the EPR spectra of all samples are that of Fe^{III}P high spin state. EPR spectra of all other prepared materials containing FeTDCSPP$(Na)_4$Cl and FeTCPP$(Na)_4$Cl shows a small amount of Fe^{III} is in high spin state, with typical g value at $\sim$6 [27,28]. A broad signal in the region of 0.1500–0.3500 T of the EPR spectra observed is attributed to Fe–Fe coupling. These are due the entrapment of porphyrin aggregates formed during the preparation of sol–gel. It is well known that charged metalloporphyrins can form these aggregates through electrostatic interaction [34,35]. The interaction between the charges in the porphyrin ring and the solid matrix can also promote a rhombic distortion of the porphyrin ring and we observe a signal at $g \sim 4.3$. Experiment 6 and 13 are the best conditions to prepare entrapped FeTDCSPP$(Na)_4$Cl, once in these conditions we do not observe the formation of aggregates or FeP with rhombic distortion. For FeTCPP$(Na)_4$Cl all conditions lead to the formation of aggregates or FeP with rhombic distortion.

SEM micrographs of silica materials loaded with FeP are presented on Fig. 3. SEM micrographs of silica trapped with FeTDCSPP$(Na)_4$Cl prepared under distinct conditions show that higher gelation temperatures (120°C) create porous structures of silicon particles irregularly assembled/aggregated (Fig. 3(a)). When gelation is carried out at room temperature the material is composed of an aggregate of larger granules (Fig. 3(b)). Silica trapped with FeTDCSPP$(Na)_4$Cl (Fig. 3(c)), FeTCPP$(Na)_4$Cl and FeTMPyP$(Cl)_5$ have heterogeneous porous and spongy structure of the silica particles. SEM image of silica loaded with FeTFPPCl (Fig. 3(d)) has a smooth surface, composed of a homogeneous aggregate of granules.

The porosity and surface properties of trapped materials containing the larger quantity of FeP were determined using nitrogen adsorption according to the BET method. The surface area, pore volume and average pore diameter of these trapped silica are presented in Table 1. The prepared materials have surface areas, between 300 and 1000 m^2/g, and pore volumes vary according to the type of FeP and conditions used in the preparation of these materials. The samples containing FeTFPPCl have a type IV isotherm pattern, according to the BDDT classification [25], indicating a larger population of pore sizes between 1.5 and 100 nm. The isotherm of xerogels containing FeTDCSPP$(Na)_4$Cl, FeTCPP$(Na)_4$Cl or FeTMPyP$(Cl)_5$ has a type II isotherm. The hysteresis loop of all materials is type H_2 according to IUPAC classification [36], normally attributed to the existence of pore cavities larger in diameter than the openings (throats) leading into them (ink-bottle pores).

5. Conclusion

In the present research it was shown that the structure and morphology of organic–inorganic hybrid materials containing FeP differ, depending on the kind of porphyrin used and the xerogel preparation conditions. The chemometric studies presented here allowed us to produce the FeP trapped materials. The use of different FeP and conditions in the preparation of xerogel lead to different product morphologies. Only FeTMPyP$(Cl)_5$ remained entrapped in the silica in all preparation conditions due the presence of cationic groups in this FeP.

In general, the negatively charged porphyrins FeTDCSPP$(Na)_4$Cl and FeTCPP$(Na)_4$Cl are entrapped in their aggregated form. Furthermore, the charged groups present in the porphyrin ring can interact with the silica structure, producing a rhombic distortion of the FeP ring. To avoid aggregation and rhombic distortion, the better condition for the entrapment of the non-charged FeTFPP is that where a smaller loading of porphyrin remains in the matrix.

Acknowledgements

Financial support from FAPESP, CAPES and CNPq are gratefully acknowledged.

References

[1] J.E. Mark, C.Y.-C. Lee, P.A. Bianconi, Hybrid Organic-Inorganic Composites, ACS Symposium Series 586, American Chemical Society, Washington, DC, 1995.
[2] P. Battioni, E. Cardin, M. Louloudi, G. Schollhorn, G.A. Spyroullias, D. Mansuy, T.G. Traylor, Chem. Commun. (1996) 2037.
[3] K.J. Ciuffi, H.C. Sacco, J.B. Valim, C.M.C.P. Manso, O.A. Serra, O.R. Nascimento, E.A. Vidoto, Y. Iamamoto, J. Non-Cryst. Solids 247 (1999) 146.
[4] K.J. Ciuffi, H.C. Sacco, J.C. Biazzotto, O.A. Serra, O.R. Nascimento, E.A. Vidoto, C.A.P. Leite, Y. Iamamoto, J. Non-Cryst. Solids 273 (2000) 100.
[5] H.C. Sacco, J.C. Biazzotto, K.J. Ciuffi, O.A. Serra, O.R. Nascimento, M.R. Zuchi, C.A.P. Leite, Y. Iamamoto, J. Non-Cryst. Solids 273 (2000) 150.
[6] K.J. Ciuffi, D.C. Oliveira, G.T. Simões, H.C. Sacco, J.C. Biazzotto, O.A. Serra, Y. Iamamoto, Boll. Chim. Farm. 138 (1999) CCLIII.
[7] Y. Iamamoto, H.C. Sacco, J.C. Biazzotto, K.J. Ciuffi, An. Acad. Bras. Ci. 72 (2000) 59.
[8] K.J. Ciuffi, H.C. Sacco, J.C. Biazzotto, M.J. Jafelicci, O.A. Serra, Y. Iamamoto, Abstr. Pap. Am. Chem. Soc. 271 (1999).
[9] D. Avnir, Acc. Chem. Res. 28 (1995) 328.
[10] G.E.P. Box, W.G. Hunter, J.S. Hunter, in: Statistics for Experimenters. An Introduction to Design, Data Analysis and Model Building, Wiley, New York, 1978.
[11] Y. Iamamoto, K.J. Ciuffi, H.C. Sacco, L.S. Iawamoto, O.R. Nascimento, C.M.C. Prado, J. Molec. Catal. A 116 (1997) 405.
[12] C.J. Brinker, G.W. Scherer, in: The Physics and Chemistry of Sol–Gel Process, Academic Press, London, 1990.
[13] S.N. Deming, in: B.R. Kowalski (Ed.), Experimental Designs: Response Surfaces in Chemometrics, Mathematics and Statistics in Chemistry, Riedel, Dordrecht, 1981.
[14] S.V. Crowder, K.L. Jensen, W.R. Stephenson, S.B. Vardeman, J. Qual. Technol. 20 (1988) 140.
[15] H. Martens, T. Naes, in: Multivariate Calibration, Wiley, Chichester, 1989.
[16] J.C. Davies, in: Statistics Data Analysis in Geology, Wiley, New York, 1988.
[17] I. Facchin, C. Mello, M.I.M.s. Bueno, R.J. Poppi, X-Ray Spectrom. 203 (1998) 15.
[18] C. Mello, J.C. de Andrade, R.J. Poppi, The Analyst 124 (1999) 1669.
[19] R.M. de Carvalho, C. Mello, L.T. Kubota, Anal. Chim. Acta 420 (2000) 109.
[20] A.R. Coscione, J.C. de Andrade, C. Mello, R.J. Roppi, B. Van Raij, M. Abreu, Anal. Chim. Acta 423 (2000) 31.
[21] B.B. Neto, I.S. Scarminio, R.E. Bruns, Planejamento e Otimização de Experimentos, Ed. UNICAMP, 1996.
[22] J.S. Lindsey, I.C. Schreiman, H.C. Hsu, P.C. Kearney, A.M. Marguerettaz, J. Org. Chem. 52 (1987) 827.
[23] A.M.A. Rocha Gonsalves, R.A.W. Johnstone, M.M. Pereira, A.M.P. Santana, A.C. Serra, A.J.F.N. Sobral, P.A. Stocks, Heterocyles 4 (1996) 43.
[24] A.D. Adler, F.R. Longo, F. Kampas, J. Kim, J. Inorg. Nucl. Chem. 32 (1970) 2443.
[25] S. Brunauer, P.H. Emmett, E. Teller, J. Am. Chem. Soc. 60 (1938) 309.
[26] G. Palmer, in: D. Dolphin (Ed.), The Porphyrins, vol. IV, Academic Press, New York, 1974 (Chapter 6).
[27] J.T. Groves, Y. Watanabe, J. Am. Chem. Soc. 110 (1988) 8443.
[28] H. H Wickman, M.P. Klein, D.A. Shirley, J. Chem. Phys. 42 (6) (1965) 2113.
[29] A. Sheldon, in: Metalloporphyrins in Catalytic Oxidations, Marcel Dekker, New York, 1994.
[30] M.D. Assis, J.R.L. Smith, J. Chem. Soc., Perkin Trans. 2 (1998) 2221.

[31] Y. Iamamoto, Y.M. Idemori, S. Nakagaki, J. Mol. Cat. A 99 (1995).
[32] C.P. Poole, in: Electron Spin Resonance: a Comprehensive Treatise on Experiment Techniques, Interscience, New York, 1967.
[33] N.M. Atherthon, in: Electron Spin Resonance Ellis Horwood Series in Physical Chemistry, Halsted, New York, 1973.
[34] K.J. Kumar, S. Balasubramanian, J. Goldberg, Inorg. Chem. 37 (1998) 541.
[35] M.A. Schiavon, L.S. Iwamoto, A.G. Ferreira, Y. Iamamoto, M.V.B. Zanon, M.D. Assis, J. Braz. Chem. Soc. 11 (2000) 458.
[36] S.J. Greg, K.S.W. Sing, Adsorption, in: Surface Area and Porosity, 2nd Ed., Academic Press, London, 1982.